Self-deployable Space Structure using Partially Flexible CFRP with SMA Wires

AKIRA TODOROKI,* KEISUKE KUMAGAI AND RYOSUKE MATSUZAKI

Department of Mechanical Sciences and Engineering, Tokyo Institute of Technology
2-12-1, O-okayama, Meguro, Tokyo 1528552, Japan

ABSTRACT: This article deals with a self-deployable composite structure using a partially flexible composite (PFC) with shape memory alloy wires and reveals the fabrication process of the PFC. Two different matrices are used in the PFC: epoxy resin for the normal part, and silicone rubber for the folding line. Since the fibers are continuous, the PFC has the same strength as a normal composite. We investigate carbon fiber breakages during the folding process by considering changes in electrical resistance, and cyclic tests are performed to confirm the availability even after long-term cyclic folding. An SMA wire is embedded in the PFC to keep the folded configuration without loading and self-deployment is achieved using Joule heating. The results confirm that a flexible part of adequate length enables foldable composite structures without causing carbon fiber breakages, while the cyclic folding tests reveal that the PFC is reliable when a long flexible part is used. The embedded SMA wire realizes compactly folded composite panel structures without loading and Joule heating of the SMA wires enables self-deployable composite structures.

Key Words: composites, SMA, self-deployable, carbon fiber, silicone rubber, epoxy.

INTRODUCTION

LAMINATED Carbon Fiber Reinforced Plastic (CFRP) is attractive as a material for aerospace structures because of its high specific strength and stiffness. In space structures especially, large lightweight structures such as solar-battery panels of tens of meters in length are required. For these large space structures, folded packaging is indispensable at the launch, and the structures are then deployed in space. Elastic–memory composites (EMC) are attractive materials for these deployable composite space structures (Francis et al., 2004; Lake and Campbell, 2004; Campbell and Maji, 2006). Another method is to use metallic hinges to construct the deployable structures, although this increases the weight. Although EMCs require a large load to fold the target composites over the glass transition temperature, they have superior convenient techniques for deployable systems. Moreover, some of the EMCs require shape memory polymers as matrix materials.

Our research group has developed a foldable composite structure for a foldable sea kayak using glass/polyester composites (Todoroki et al., 2008). Two kinds of matrix are used in the material: normal thermoset resin such as epoxy for the greater part of the structure and silicon rubber for the fold line. This material is called a partially flexible composite (PFC). The PFC can very easily be folded with only a small force. Since the carbon fibers are continuous throughout the structure, the PFC has perfect stiffness and strength except for the fold line. For the fold line, a different stiffener is used in the sea kayak.

In the present study, Shape Memory Alloy (SMA) wires are embedded in the flexible part of the PFC. These SMA wires have a straight shape memory. Since the flexible part is made from a soft matrix, the PFC can easily be bent by a small force. Plastic deformation of the embedded SMA wire keeps the shape of the folded CFRP structure. When the temperature of the PFC with embedded SMA wires is elevated to the shape recovery temperature of the SMA wires, the SMA returns to a straight shape and this deploys the CFRP structure. This means that a PFC with embedded SMA (PFC-S) has the ability to self-deploy when the temperature of the structure increases to the shape recovery temperature of the SMA. The PFC-S requires no expensive material. Since a flexible composite is used at the folding line, only a small force is required to fold the PFC-S without the need for increased temperature.

In this study, we describe the process of creating the PFC-S and evaluate experimentally the minimum curvature of the PFC-S to prevent fiber breakages. Since the length of the flexible part significantly affects

*Author to whom correspondence should be addressed.
E-mail: atodorok@ginza.mes.titech.ac.jp
Figures 2 and 4 appear in color online: http://jim.sagepub.com

1045-389X/09/12 1415–10 $10.00/0 DOI: 10.1177/1045389X09337086

the minimum curvature for preventing fiber breakages, several lengths are investigated. Since embedding SMA wires causes an increase in stiffness of the flexible part of the PFC-S, the nominal bending stiffness is measured with a three-point bending test. Plastic deformation of the SMA wire impedes spring back of the PFC from the folded shape. In the present study, feasibility of the foldable PFC-S is investigated experimentally using several different PFC-S materials. After concluding these tests, a large prototype PFC-S is fabricated, and the embedded SMA wires are heated using a Joule heating process in an attempt to model a self-deployable space antenna.

PFC FABRICATION PROCESS

Figure 1 shows a schematic representation of the process to make a PFC. A PFC comprises two kinds of matrix. For the main part an epoxy resin is used as matrix and this has the same high stiffness as a normal CFRP. The flexible part uses silicone rubber as matrix. Fabric carbon cloth fibers are adopted as the reinforcement material with the carbon fibers continuous throughout the entire plate.

First, the silicone rubber is painted onto the designated folding line of the fabric carbon cloth. This study uses normal carbon cloth W1103-1K (Toho Tenax Co., Ltd) for reinforcement and normal silicone rubber (S45, acid-free oxime type cross-linker, Shin-Etsu Chemical Co., Ltd) as the matrix at the folding line. Since the silicone rubber is cured at room temperature, no additional treatment is required for the silicone rubber matrix. Then, another fabric carbon cloth is stacked on the initial ply, and the silicone rubber is once again painted onto the same part of the designated folding line. This process is repeated until the number of plies reaches the designated thickness. After the silicone rubber has been applied, normal epoxy resin is infused into the rest of the plate. We use normal epoxy resin that cures at room temperature (type Z2/H07, Nissin Resin Co., Ltd) in this study. After 24 hours of curing at room temperature the plate becomes a PFC, which can be bent at the flexible part as shown in Figure 2.

The silicone rubber in the PFC has several roles: it prevents the epoxy resin from infusing into the folding line, it protects the carbon fibers and it supports the carbon fibers mechanically. This type of silicone rubber is durable at high temperatures like 150°C and tough against humidity. The silicone rubber is elastic even at low temperatures like −50°C.

The silicone rubber has good bonding strength to the epoxy resin. Figure 3 shows a cross-section photograph at the interface between the epoxy resin and silicone rubber of the PFC. As shown in Figure 3, there is no obvious interface boundary. To check the bonding

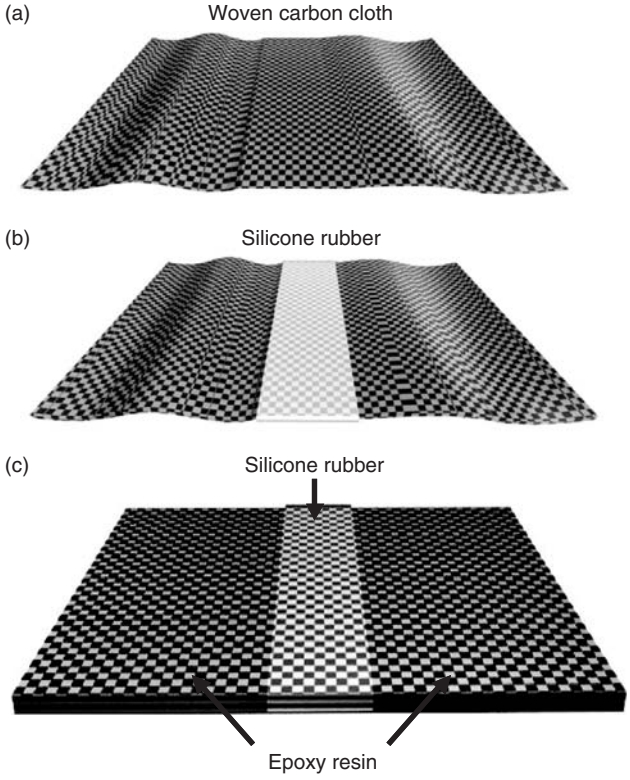

Figure 1. *Fabrication process of partially flexible composites: (a) Woven carbon cloth, (b) Painting of silicone rubber, and (c) Epoxy resin impregnation.*

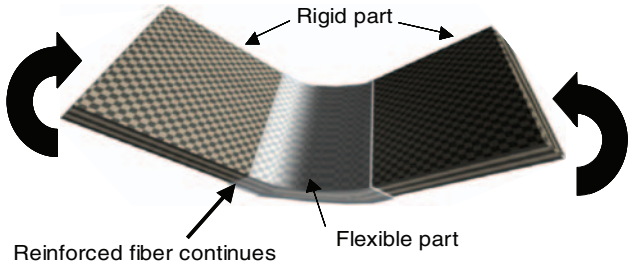

Figure 2. *Bending of partially flexible composites.*

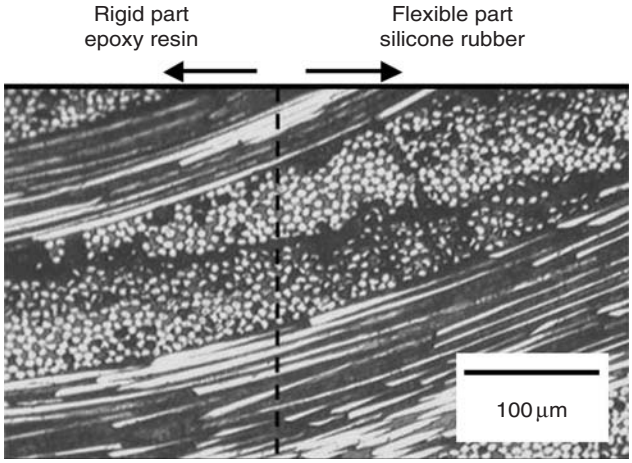

Figure 3. *Cross section of flexible folding line.*

strength to epoxy, tensile tests were performed using epoxy-silicone rubber specimens as shown in Figure 4. Both ends of a specimen are made from epoxy and the middle is made from silicone rubber. As shown in Figure 4, the fracture always occurs in the middle of the silicone rubber region. This means that the bonding strength is higher than the tensile strength of the silicone matrix.

Tensile tests were performed using rectangular specimens as shown in Figure 5. The middle of the specimen is flexible, while both ends are rigid epoxy matrix composites. The tensile test results are shown in Figure 6 together with comparisons with the tensile strength of normal CFRP. The left bar shows the averaged values of the results of normal CFRP, while the right bar shows the averaged values of the results of the PFC. In both cases, 15 tests were performed. Figure 6 shows that the PFC has the same tensile strength, although all PFC specimens broke at the flexible part. The continuous carbon fibers through the rigid part to the flexible part maintain the high tensile strength of the PFC.

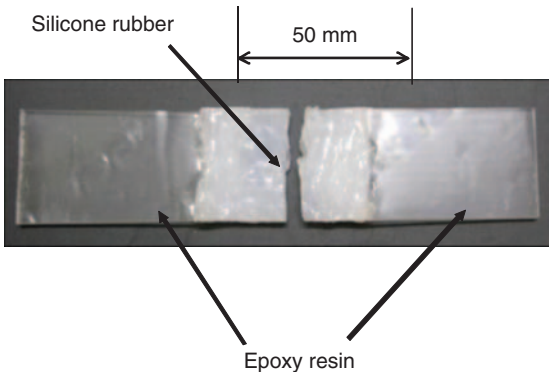

Figure 4. *Resin bonding test specimen after tensile test.*

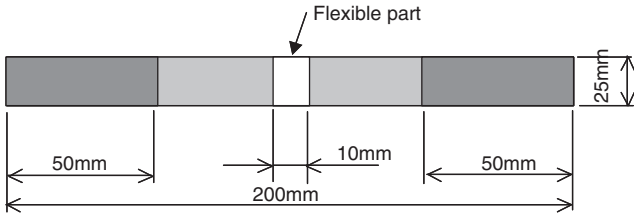

Figure 5. *Tensile test specimen of PFC.*

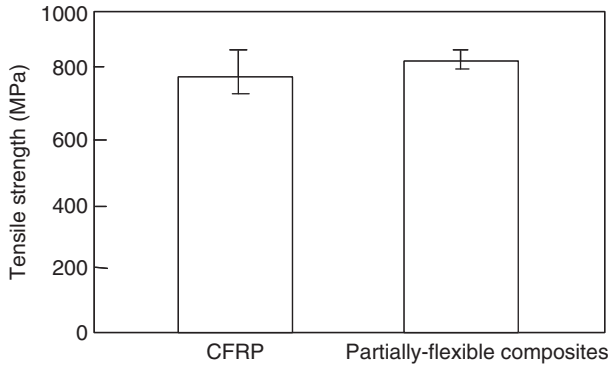

Figure 6. *Comparison of results of tensile strength.*

DETECTION OF FIBER BREAKS DURING BENDING

Test Method

To investigate the bending curvature without causing a fiber break, eight plies of carbon fabric cloths of CFRP are used, together with four different lengths for the flexible part; the lengths being 2, 3, 4, and 5 mm. The dimensions of each specimen are 180 mm long and 50 mm wide, while the thickness of the specimen is ~1 mm. To detect carbon fiber breakages, the electrical resistance of the specimen is monitored during the bending process. Two copper foil electrodes are attached and co-cured to measure the electrical resistance change during the epoxy resin infusion process. Since fabric cloth CFRP has isotropic electric properties in the fabric cloth plane, electrical contact at the copper foil is not a significant process here. The fabric cloth CFRP has smaller electric conductivity in the thickness direction, and the smaller electric conductivity may cause different electric currents in the thickness direction compared to isotropic materials such as metal. To investigate the electric current, the electric potential of the upper and bottom surfaces is measured and the electric current is found to be approximately uniform in the flexible part when spacing between the copper electrodes is 80 mm.

We constructed a new apparatus to measure the electric voltage change and curvature of the PFC as shown in Figure 7. Two wooden plates are attached using metallic hinges and a potential meter is attached at the corner. The angle between the plates is measured

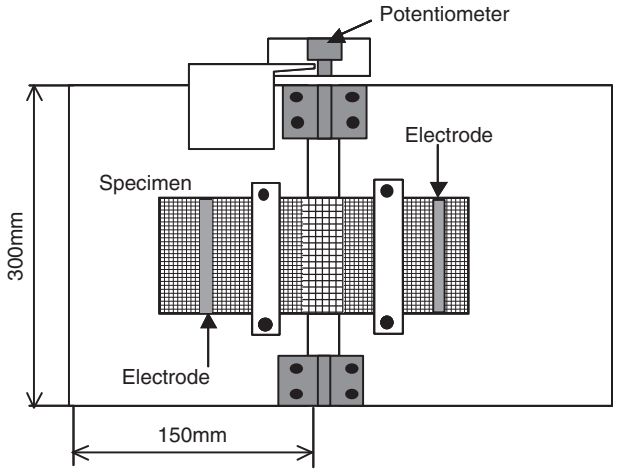

Figure 7. *Bending apparatus for PFC with electrical resistance change method.*

using the potential meter and a constant electric current of 0.7 (A) is applied to the specimen. After measuring the relationship between the electric voltage of the potential meter and the angle of the plates, we performed tests to measure the change in electric resistance of the specimen during bending. The results from a typical test, in which a PFC specimen with a 2 mm wide flexible part is bent and the electrical resistance measured, are shown in Figure 8. The abscissa is the bending angle and the ordinate the electrical resistance. As shown in Figure 8, electrical resistance increases rapidly at an angle of ~35°. This means that fiber breaks occur at a bending angle of 35° for a PFC specimen with a 2 mm wide flexible part.

Although the curvature of the specimen is not exactly uniform, it can be approximately calculated using the assumption of uniform curvature. When the curvature (κ) of the flexible part is uniform, the specimen curvature radius ρ is defined as shown in Figure 9. In this process, since the length of the flexible part is sufficiently large compared to the thickness, curvature is assumed to be uniform throughout the flexible part. From the measured rotation angle (θ) at which the carbon fibers break and the length of the flexible part (x), the practical maximum curvature without a carbon fiber break is calculated as

$$\kappa = \frac{1}{\rho} = \frac{\theta}{x} \tag{1}$$

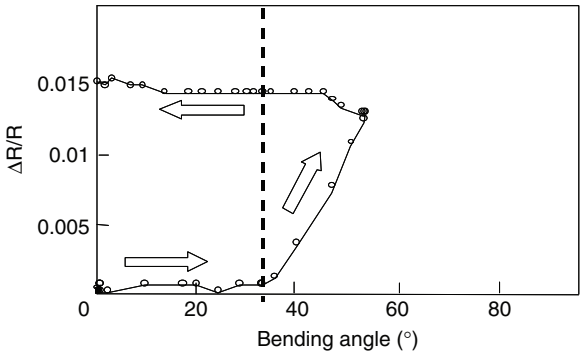

Figure 8. *Electrical resistance change during bending of specimen with 2 mm flexible length.*

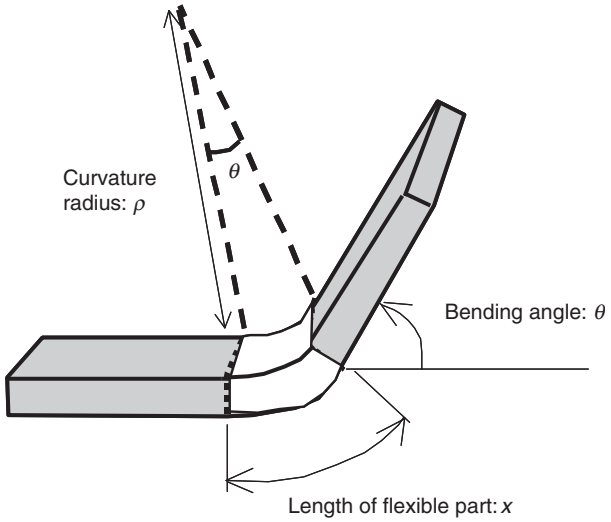

Figure 9. *Definition of bending curvature radius.*

Results and Discussion

The measured curvatures at which a fiber breakage occurs are shown in Figure 10. The abscissa is the length of the flexible part and the ordinate the measured curvature when the fiber breaks. As shown in Figure 10, the measured curvature at which the fiber breakages occur is almost constant. The multiple of half the thickness to the curvature produces the maximum bending strain. This means that the fiber breaks at a constant applied strain.

Figure 10 shows that a longer flexible part enables foldable composite structures to be constructed, although the elastic spring back makes it difficult to keep the folded configuration. This is remedied by embedding SMA wires in the PFC and is described in a later section.

Cyclic Bending Test

For space structures, the folding and deployment process is repeated several times including tests on the ground. To confirm the repeatability of this process, cyclic bending tests were performed using the test apparatus shown in Figure 7. Half the PFC plate is bent up to 90°. The cyclic process is performed using a motor attached to the apparatus. The cyclic speed is 2 Hz and the number of cycles is counted using the potential meter.

The specimens for the cyclic bending test are similar to those used in the static bending test mentioned previously; the material used is eight-ply fabric cloth CFRP. Each specimen is 1 mm thick, 150 mm long, and 25 mm wide. Several different lengths for the flexible

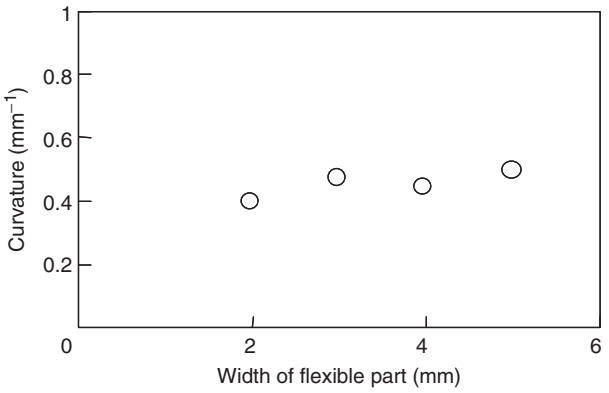

Figure 10. *Measured fiber breakage curvature of various flexible part lengths.*

part of the specimen are used: 2, 4, and 10 mm. A couple of copper foil electrodes, each with a thickness of 0.02 mm, are co-cured on the surface of each specimen. In this cyclic test, fiber breakages are investigated during 10^5 cycles. The fiber breaks are identified by the electrical resistance changes as previously described for static bending.

Figure 11 shows the measured fiber breakages during cyclic bending. The abscissa is the number of cycles and the ordinate the fiber breakages (%) identified by changes in electrical resistance. In the cyclic bending test, the hinge part is bent mechanically without considering the uniform curvature. This may cause fiber breakages even in larger flexible parts. The results show that most of the fiber breakages occur during the earlier cycles. After a fiber breakage in the initial cycles, the increase in fiber breakages is very slow until the life limit cycle of 10^5. For example, for a specimen with a 2 mm length flexible part, half the carbon fibers break at the first bending, but the fiber breakages do not increase until after 10^5 cycles. For a specimen with a 10 mm length flexible part, the fiber does not break before 5×10^4 cycles.

This indicates that the first bending cycle is very important and if we select the length of the flexible part adequately to prevent fiber breakages during the first bending cycle, we do not need to concern ourselves with fiber breakages for many additional cycles. For a self-deployable structure, the required number of bending cycles is 10^2 at most including tests on the ground.

IMBEDDING SMA WIRE

Process to Embed SMA Wire

The PFC itself cannot maintain the bent configuration because the carbon fibers have elastic spring back energy at bending. To keep the folded configuration, we need metallic wires that plastically deform to the folded shape and resist the spring back of the carbon fibers. When SMA wire with a straight shape memory is embedded into the folding line of the PFC, the PFC with the SMA wire maintains a folded configuration because of the plastic deformation of the SMA wire and the structure returns to a straight shape when heated to the characteristic phase transformation temperature.

In this study, commercially available SMA wire (Ti–Ni alloy) with a straight shape memory is used. The diameter of the wire is 1 mm, and the phase transformation temperature 80°C. The procedure for creating a PFC-S (PFC with SMA wire) is as follows:

(1) Paint silicone rubber on the folding line of the carbon fabric cloth ply.
(2) Place the next ply.
(3) Stack and paint the silicone rubber until the number of plies is half the planned number.
(4) Place straight SMA wire as shown in Figure 12. The length of the SMA wire is 20 mm longer than the length of the flexible part.
(5) Stack the rest of the plies and paint the silicone rubber.
(6) Infuse epoxy resin into the normal part where there is no silicone rubber.
(7) Cure at room temperature for 24 hours.

The finished specimen is shown in Figure 12.

As shown in Figure 12, the SMA wire is embedded in the center of the thickness here. The reason is to keep the flexible part foldable in the present study. When users want to increase the stiffness of the flexible part, they should embed the SMA wire in the outer layers. When the SMA wire is attached on the PFC surface, the increase of the stiffness is maximized: this means the decrease of the flexibility.

Tests for Foldable Configuration

As mentioned previously, the PFC-S maintains its folded configuration. The folded carbon fibers of the PFC tend to spring back to a straight configuration, but the plastically deformed SMA wire prevents this from happening.

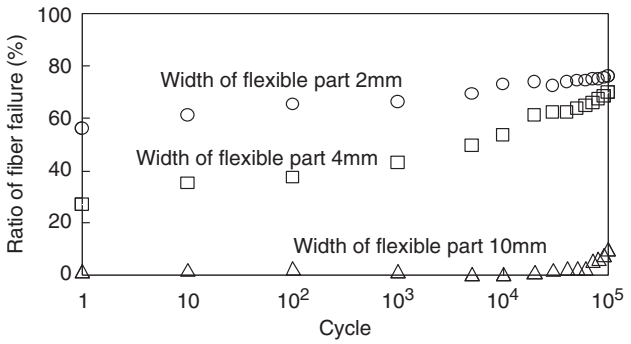

Figure 11. *Results of cyclic bending test.*

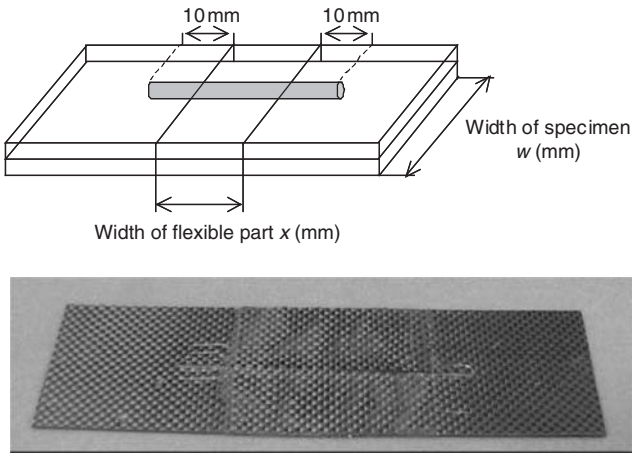

Figure 12. *PFC with SMA wire.*

The ability to maintain a folded configuration, however, depends on the stiffness of the embedded SMA wire and the spring back effect of the carbon fiber. This means that the folded configuration may change due to the width of the specimen and due to length of the flexible part: a longer specimen implies a greater elastic spring back.

In the present study, we used three different lengths for the flexible part: 10, 50, and 100 mm. Three different specimen widths were selected for the test: 40, 60, and 80 mm. The specimen width determines the spacing between adjacent SMA wires in practice. In this test, the specimen is statically bent and the flexible part is uniformly bent to obtain uniform curvature. Figure 13 shows the results of the folded configuration without external support. The curvature is measured assuming uniform curvature in the flexible folding line.

Figure 14 shows the results of the minimum curvature. The abscissa is the specimen width and the ordinate the specimen minimum curvature. The solid circles depict the results of using specimens with a 10 mm flexible length; the solid square symbols depict the results of using 50 mm flexible lengths while the solid triangular symbols depict the results of using 100 mm flexible lengths. These results indicate that the spring back effect increases with an increase in the specimen width (spacing between SMA wires) and the length of the flexible part. This means that the total area of the flexible part has a significant effect on the spring back of carbon fibers. Since the tests are performed with a constant thickness specimen, the effect of the specimen thickness cannot be determined as yet. A cross section image of the flexible part, shown in Figure 15, indicates that the bonding between the SMA wire and the silicone rubber is good and that no fiber breakages are observed here.

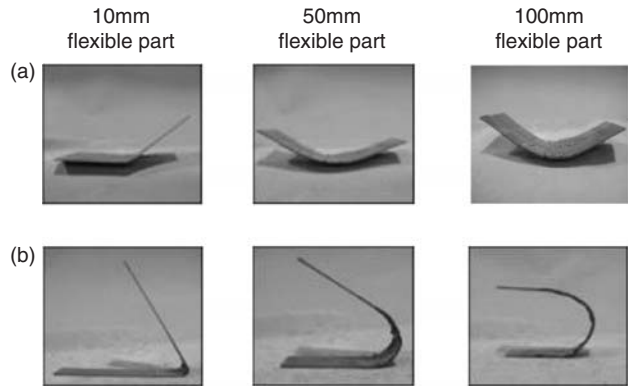

Figure 13. *Folded specimen configurations at completely unloaded condition of various dimensions: (a) Width of specimen = 80 mm and (b) Width of specimen = 20 mm.*

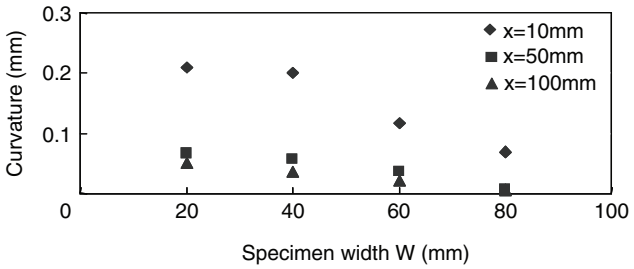

Figure 14. *Minimum curvatures of the various widths.*

BENDING STIFFNESS OF PFC-S

Bending Stiffness Model

For practical applications such as antennas or solar panels, high stiffness is required to prevent undesired vibration. To obtain the designed bending stiffness of the PFC-S structure, a simple model to predict bending stiffness of the PFC-S is useful. We constructed a simple model to predict the equivalent bending stiffness of the PFC-S and compared the performance thereof with the experimental results.

Figure 16 illustrates the simple model, in which the specimen is divided into three regions: a normal CF/epoxy composite part with no embedded SMA wire; a normal CF/epoxy part containing an embedded SMA wire; and a flexible part with a silicone rubber matrix and containing an embedded SMA wire. The equivalent bending modulus and geometrical moment of inertia of the three parts are expressed as (E_1, I_1), (E_2, I_2), and (E_3, I_3).

The second (E_2, I_2) and third (E_3, I_3) parts that contain embedded SMA wires, are divided into two parts in the cross sections: the area that does not include a SMA wire and the area that does. Let us consider that the second and third parts are SMA wire reinforced composites: reinforcement is the SMA wire and the matrix is the CF/epoxy or CF/silicone rubber composites. Let the bending modulus of the area that does not include a SMA wire be E_n and the bending modulus of the SMA wire be E_s: E_n is then equal to the bending modulus of the CF/Epoxy. The bending modulus of the area that includes a SMA is calculated using the elastic

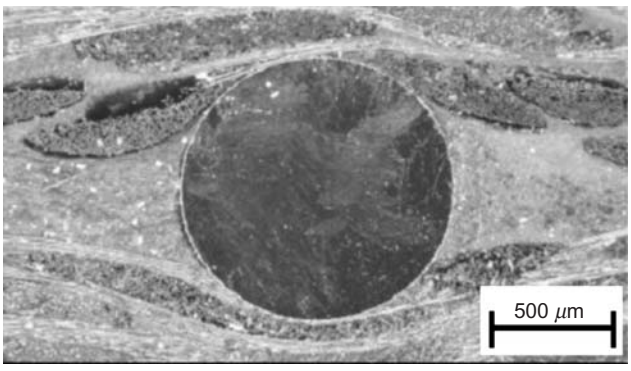

Figure 15. *Cross section of SMA wire after the first bending.*

modulus of the SMA wire E_S according to the rule of mixture:

$$E_M = \frac{\pi(a/2)^2}{aw} E_s + \frac{aw - \pi(a/2)^2}{aw} E_n \tag{2}$$

where a is the diameter of the SMA wire and w the width of the specimen.

In the part that does not include a SMA wire, the carbon fibers are twisted as a result of the existence of the SMA wire in the middle of the cross section. The effect of the twisted fibers can be included by using the empirical correction factor k. The elastic moduli E_2 and E_3 are obtained from the rule of mixture:

$$E_2, E_3 = \frac{2b}{a+2b} k E_{\text{matrix}} + \frac{a}{a+2b} E_M \tag{3}$$

The factor k is introduced to correct the effect of carbon fiber undulation due to the existence of the SMA wire (Tsai, 1964). The k is selected to fit the experimental results.

As mentioned previously,

$$E_1 = E_n \tag{4}$$

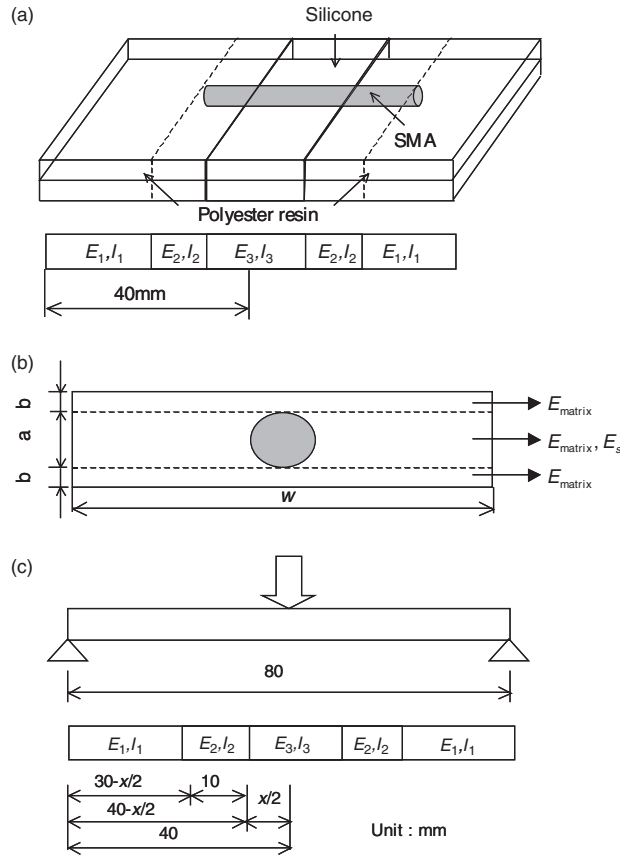

Figure 16. *Equivalent bending elastic modulus model: (a) Specimen model, (b) Bending elastic modulus model, and (c) Configuration of 3-point bending test.*

Geometrical moments of inertia of the parts that include SMA wires, I_2 and I_3, are calculated from the equivalent moments of inertia as follows:

$$I_2, I_3 = \int_{-a/2}^{a/2} y^2 \frac{E_M}{E_n} w \mathrm{d}y + 2\int_{a/2}^{a/2+b} y^2 w \mathrm{d}y \tag{5}$$

The geometrical moment of inertia of the part that does not include a SMA wire can be calculated as follows:

$$I_1 = \int_{-a/2-b}^{a/2+b} y^2 w \mathrm{d}y \tag{6}$$

Using these three elastic moduli and the geometrical moments of inertia, the elastic modulus for the three-point bending test of the PFC-S can be calculated. The span length of the three-point bending test is 80 mm and the length of the flexible part is x mm. The maximum displacement at the middle loading point can be calculated as follows:

$$y = \frac{32000P}{3E_3I_3} - \frac{(40 - x/2)^3 P}{6}\left(\frac{1}{E_3I_3} - \frac{1}{E_2I_2}\right) - \frac{(30 - x/2)^3 P}{6}\left(\frac{1}{E_2I_2} - \frac{1}{E_1I_1}\right) \tag{7}$$

Experimental Investigation

To validate the model before calculating the bending modulus, we performed three-point bending tests on the PFC-S. The specimen used was 100 mm long, 40 mm wide, and 1.25 mm thick. We prepared two different lengths for the flexible part: 10 mm and 50 mm. A material testing machine, Type AG-I100KN and made by Shimazu Co. Ltd. was used according to the Japanese three-point bending test standard, JISK7074.

Load–displacement curves are obtained from the experimental results and the equivalent elastic modulus is calculated as follows:

$$E = \frac{L^3 P}{4bh^3\delta} \tag{8}$$

where L is the span length (80 mm), b the specimen width (40 mm), h the specimen thickness (1.25 mm) and P/δ the slope of the initial linear part of the load–displacement curve. All the elastic moduli and geometrical moments of inertia used in the calculations are listed in Table 1. The equivalent bending moduli in Equation (8) were obtained from the calculated

Table 1. Bending elastic modulus and polar moment of inertia of area (partially flexible CFRP with SMA embedded).

	PFF-1S	PFF-2S
$E1$ (GPa)	8.51	8.51
E_2 (GPa)	12.31	13.69
E_3 (GPa)	3.06	3.44
I_1 (m^4)	6.51×10^{-12}	6.51×10^{-12}
I_2 (m^4)	6.76×10^{-12}	6.78×10^{-12}
I_3 (m^4)	6.83×10^{-12}	6.91×10^{-12}

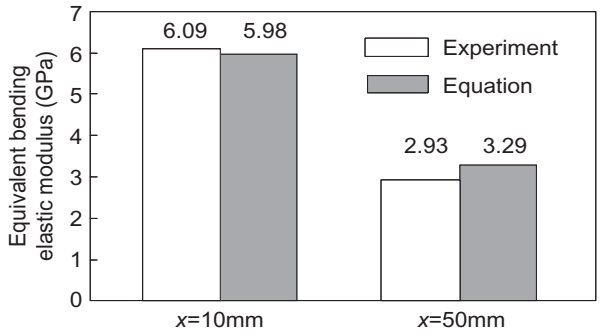

Figure 17. *Comparison of experiment and analytic equation in partially flexible CFRP with SMA embedded.*

load–displacement slope. According to the results shown in Figure 17, the calculated equivalent elastic bending modulus in both cases is almost equal to the measured results. These results show that the elastic modulus of the PFC-S can be calculated using Equation (7). Thus using Equation (7), we can design the required spacing and/or diameter of the embedded SMA wires to obtain the required elastic stiffness of the PFC-S for a practical structure.

TEST OF SELF-DEPLOYABLE STRUCTURE

As a feasibility study, we constructed a small desktop model of a self-deployable structure using the PFC-S. Figure 18(a) shows the schema of this model. The stacking sequence of the specimen is $[(0/90)_8]$: eight plies of woven fabric cloth are stacked in an identical orientation. The dimensions of the specimen are 1000 mm in length, 300 mm in width, and with a 1.25 mm thickness. The composite panel has four flexible parts equally spaced. The length of a flexible part is 100 mm. Eight SMA wires are embedded with a spacing of 40 mm. To elevate the temperature of the SMA wires using a simple Joule heating method, eight

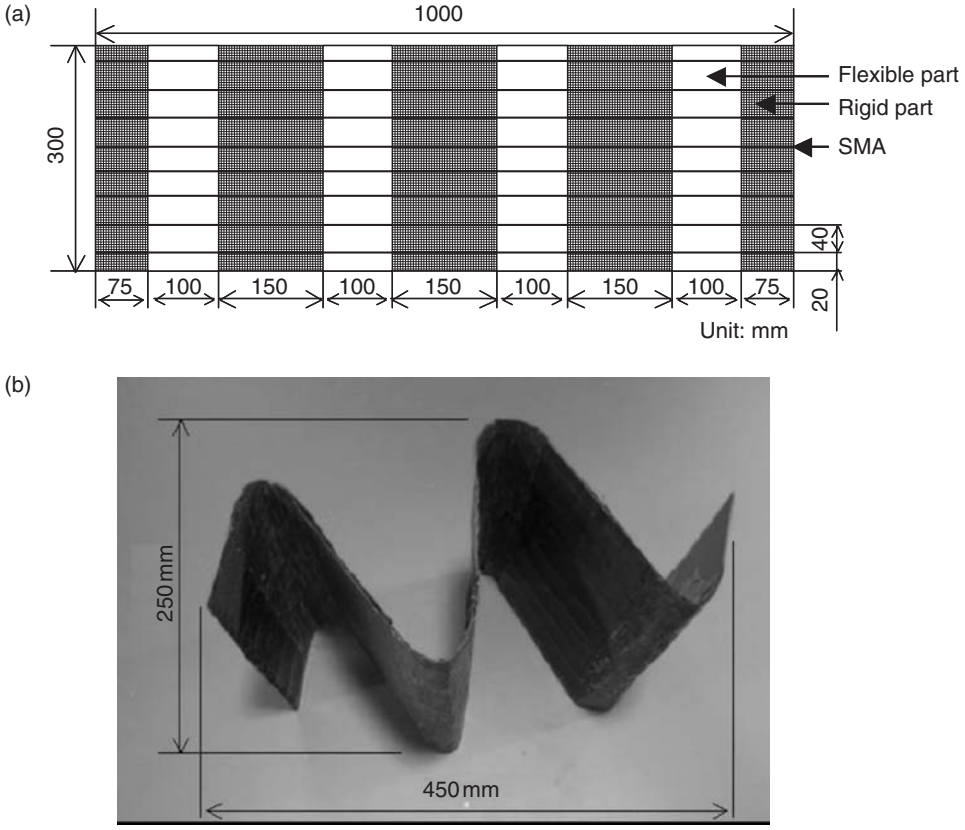

Figure 18. *Self-deployment structure model: (a) Configurations of specimen and (b) Folded type.*

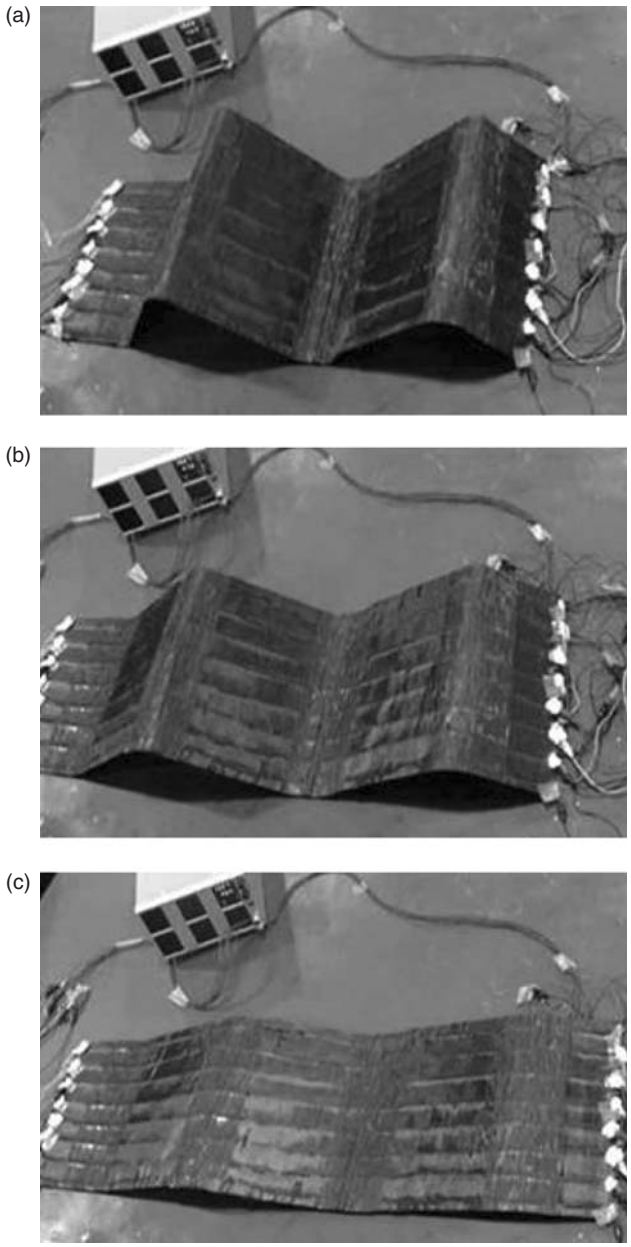

Figure 19. *Deployment of self-deployment structure model: (a) 2 s, (b) 6 s, and (c) 14 s.*

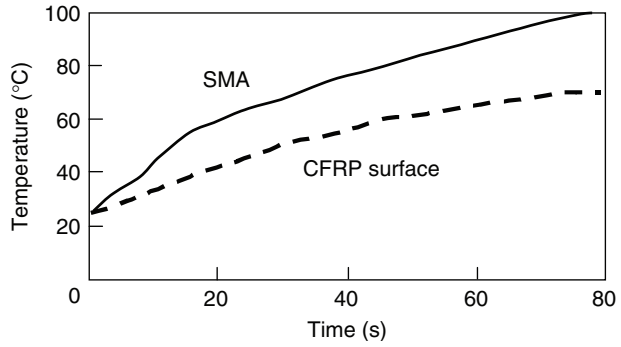

Figure 20. *Temperature change due to Joule heating.*

110 mm long SMA wires are used and the extra 5 mm at either end is used for electrodes.

Figure 18(b) shows the folded type specimen. Each flexible part is folded at a curvature of 0.034 (1/m) and the plastic deformation of the SMA wires ensures that the folded configuration is maintained without loading. The folded panel can be stored in a small pack 250 mm long, 300 mm wide, and 450 mm high. The eight SMA wires are connected in parallel, and a direct current of 45 (A) is applied using a stable electric current supply. The deployment process is shown in Figure 19. Figure 20 shows the measured temperature on the specimen surface during heating. The abscissa is the time from the start of Joule heating and the ordinate is the temperature measured using thermocouples. The temperature of the SMA wires shows that the direct electric current applied to the SMA wires causes Joule heating and the temperature of the SMA wire exceeds the shape recovery temperature (80°C). Since the thermocouple is attached to the SMA wire with electric insulation tape, the measured temperature is lower than the actual temperature. The difference in temperature between the SMA wire and composite surface means that the electric current flows mainly through the SMA wire. Measurements of the electric voltage at several points on the composite surface indicate that almost all the electric current flows through the SMA wire. This may enable us to estimate the required electric current for deployment in our future research.

CONCLUSIONS

This article deals with a self-deployable composite structure using a PFC with SMA wires. The article reveals the fabrication process of the PFC and the fiber breakages during the folding process. A SMA wire is embedded in the PFC to maintain the folded configuration without loading until self-deployment using a Joule heating method. The results obtained are summarized below.

(1) Using epoxy resin and silicone rubber as the matrices of the composite structure, a partially flexible composite, that is easily folded with a small force, can be developed.
(2) If the flexible part is sufficiently long, no fiber breakage occurs during the folding process.
(3) Embedding a SMA wire in the flexible part enables the folded configuration to be maintained without loading as a result of the plastic deformation of the SMA wire.
(4) Joule heating of the SMA wire enables self-deployment of the composite structure.

REFERENCES

Campbell, D. and Maji, A.K. 2006. ''Failure Mechanisms and Deployment Accuracy of Elastic-Memory Composites,'' *Journal of Aerospace Engineering*, 19(3):184–193.

Francis, W., Lake, M., Hinkle, J. and Peterson, L. 2004. ''Development of an Elastic Memory Composite Self- Locking Linear Actuator for Deployable Optics,'' In: *Proceedings of the 45th SDM Conference AIAA*, AIAA 2004-1821, Palm Springs, California.

Lake, M. and Campbell, D. 2004. ''The Fundamentals of Designing Deployable Structures with Elastic Memory Composites,'' In: *Proceedings of IEEE Aerospace Conference*, #1134, USA.

Todoroki, A., Kumagai, K. and Matsuzaki, R. 2008. ''Foldable GFRP Boat Using Partially Flexible Composites,'' In: *Proceedings of the SAMPE Fall Technical Conference: Multifunctional Materials: Working Smart Together*, Memphis, TN, USA, September 8–11, Society for the Advancement of Material and Process Engineering, CD-ROM-6.

Tsai, S.W. 1964. ''Structural Behavior of Composite Materials'', NASA CR-71.